

Communication

High Brightness Diode Lasers Based on Beam Splitting and Polarization Combining

Yufei Zhao ¹, Cunzhu Tong ^{2,*}, Lijie Wang ², Yanjing Wang ², Huanyu Lu ², Xin Zhang ², Zhipeng Wei ^{1,*} and Lijun Wang ²

¹ Key Laboratory of High Power Semiconductor Lasers, School of Physics, Changchun University of Science and Technology, Changchun 130022, China

² State Key Laboratory of Luminescence and Applications, Changchun Institute of Optics, Fine Mechanics and Physics, Chinese Academy of Sciences, Changchun 130033, China

* Correspondence: tongcz@ciomp.ac.cn (C.T.); weizp@cust.edu.cn (Z.W.); Tel.: +86-0431-86176349 (C.T.); +86-0431-85583390 (Z.W.)

Abstract: A new method to improve the brightness of diode lasers based on beam-waist splitting and polarization combining was proposed and demonstrated. The beam waist was split by a precisely cut prism into two parts and combined with a polarization beam combiner. The advantages of simple setup, high efficiency, brightness, and universality were presented. The slow axis M^2 factor of a broad-area diode laser with a ridge beam width of 180 μm was reduced from 18.5 to 9.8, and a brightness of 42.4 $\text{MW cm}^{-2} \text{sr}^{-1}$ was realized; this brightness was a 84.21% improvement of the same emitter at 8 A. The slow axis M^2 factor of a commercial broad-area diode laser array combined by spectral beam combining was reduced from 9.08 to 4.78, and 80.6% improvement of brightness was realized on the same commercial broad-area diode laser array. A brightness of 195.8 $\text{MW cm}^{-2} \text{sr}^{-1}$ was realized at 36 A by this diode laser array. This method can be applied in a highly polarized light source to improve the beam quality and brightness.



Citation: Zhao, Y.; Tong, C.; Wang, L.; Wang, Y.; Lu, H.; Zhang, X.; Wei, Z.; Wang, L. High Brightness Diode Lasers Based on Beam Splitting and Polarization Combining. *Appl. Sci.* **2022**, *12*, 7980. <https://doi.org/10.3390/app12167980>

Academic Editor: Edik U. Rafailov

Received: 24 June 2022

Accepted: 8 July 2022

Published: 9 August 2022

Publisher's Note: MDPI stays neutral with regard to jurisdictional claims in published maps and institutional affiliations.



Copyright: © 2022 by the authors. Licensee MDPI, Basel, Switzerland. This article is an open access article distributed under the terms and conditions of the Creative Commons Attribution (CC BY) license (<https://creativecommons.org/licenses/by/4.0/>).

Keywords: high brightness; diode; beam combining

1. Introduction

High-power diode lasers present great advantages in many applications, such as pumping solid-state lasers or fiber lasers, medical treatment display technology, and material processing, especially additive manufacturing [1–10]. The main advantages of such lasers are high energy-conversion efficiency, small size, electric drive, long lifetime, and relatively low cost. However, the beam-quality of diode lasers is still poor and the brightness is low due to the narrow cavity and broad-area (BA) waveguide of a single diode laser. Progress on the beam quality of BA lasers will have significant potential effects on the development of related fields.

The beam quality of a diode laser can be described as the product of divergence angle and beam waist [11], and the brightness is defined as the ratio of power and beam quality [12]. Beam combining methods, such as spectral beam combining (SBC) [13–15], polarization beam combining, and coherent beam combining (CBC) [16–18], are able to enhance the brightness of lasers system via combining more laser elements to increase the power. However, the beam quality of SBC is limited by the emitters and the output coupler, and diffraction grating brings inevitable power loss. CBC with low efficiency is complex and sensitive to the environment, which limits the application in many fields. It is difficult to improve the beam quality except for the external-cavity beam combining.

In this paper, we demonstrated a new approach to improve the beam quality and brightness of diode lasers based on the beam-waist splitting and polarization combining (BSPC). The beam-waist was cut in half via the splitting prism, and one of the cut beam's polarizations was changed by a half-wave plate. These two beams, with different

polarizations, were combined into one beam by PBC [19]. This system can realize the improvement of beam quality by shrinking the beam-waist. This method was applied for the single BA diode laser and laser bar, and the improvement of beam quality and brightness was investigated.

2. Materials and Methods

Beam quality of a semiconductor laser can be described by the M^2 factor, which is defined as

$$M^2 = \frac{w \times \theta}{w_0 \times \theta_0}, \quad (1)$$

where w and θ are, respectively, the diameter of the measured beam waist and the far-field divergence. w_0 and θ_0 are, respectively, the diameter of the TEM₀₀ Gaussian beam waist and the far-field divergence. The beam width was determined by the second-order moment according to ISO11146. A small M^2 factor value is desired for high-power diode lasers. Evidently, the beam quality can be improved by reducing the beam waist when the divergence angle is constant.

Figure 1 shows the schematic of experimental setup of BSPC. A laser beam from the diode laser was split into two beams by a triangle prism along the beam waist in slow axis, and then these two beams went through two loops to overlap on a polarization beam combiner (PBC) using high reflecting mirrors. The polarization of one beam was changed by a half-wave plate (HWP). These two beams were combined into one beam by PBC. In principle, the beam quality of a single beam would improve by 50% because the beam-waist was reduced to its half, and the power would be almost unchanged due to the combining if the initial laser beam has a high purity polarization. Hence, the brightness increases. This method is suitable for the laser source with high purity polarization and large beam waist. Additionally, this approach improves the brightness with the penalty of polarization purity. To demonstrate this method, a single emitter and a diode laser array are employed.

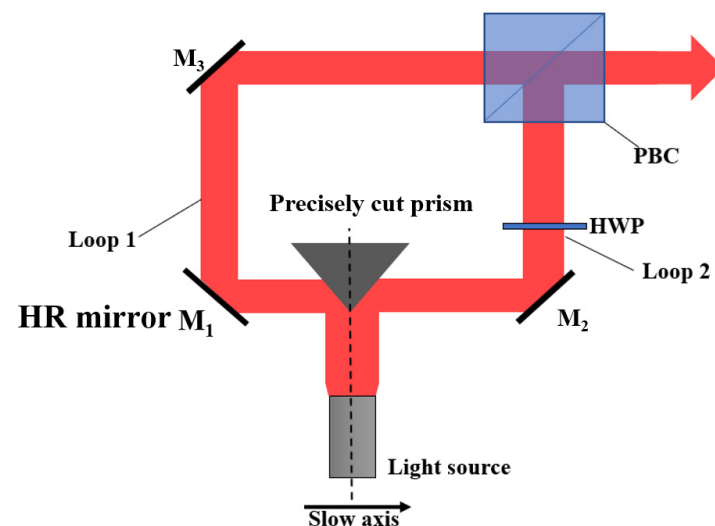


Figure 1. Schematic diagram of BSPC setup. HR mirror: highly reflective mirror, PBC: polarization beam combiners, HWP: half-wave plate.

In the realistic setup, the highly reflective (HR) mirrors (M_1 , M_2 , M_3) were optical glass coated with Au. The corresponding reflectivity was 98.2%, and the size was 30 mm × 30 mm × 10 mm. The HWP used was zero-order with a transmission of 98.5% at 980 nm. The precisely cut prism, manufactured from N-BK7, featured reflective coatings on the two legs and offered a clear aperture extending across the 90° angle between the coated surfaces. The combining efficiency of the PBC was 97.5%.

3. Results

3.1. BSPC of Single BA Diode Laser

A 980 nm BA diode laser with a ridge beam width of 180 μm was used as the light source for BSPC, which was put on a water-cooled plate with a water temperature of 20 $^{\circ}\text{C}$. Figure 2 shows the power curves of the laser before combining (black balls) and after BSPC (red balls) under CW operation. The power was measured by Ophir FL500A. As can be seen, the output power of the laser under free running was 6.78 W at 8 A, and the electro-optic conversion efficiency of the laser was 51.2%. The corresponding power for BSPC was 6.13 W at the same driven current, which was approximately 9.5% lower than that of the same laser at free running. The reason for the power reduction was because the polarization of the laser was not pure enough, resulting in the loss in PBC. In addition, the power loss was partly due to the insufficient reflectivity of M_1 , M_2 , and M_3 and the precisely cut prism. The inset in Figure 2 shows the far-field spots before and after BSPC at 6 A. It can be seen that the spot shape of the laser with BSPC was asymmetric and exhibited a much narrower lateral far-field pattern, which enabled the improvement of beam quality. The inset is the far field of before and after BSPC. It can be seen that the shape after the BSPC's far field was asymmetric and like a shield. The reason for the asymmetric shape was that the original laser was separated from the middle of the beam. The power in the middle of the original beam was higher than that at the edge. The separated edge became blurred due to the diffraction effects of the triangle prism.

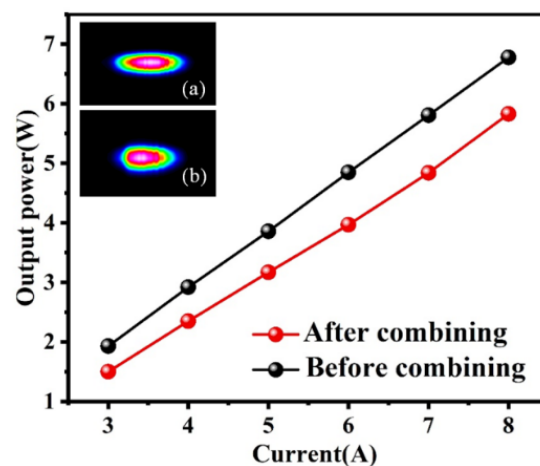


Figure 2. Power characteristics of a single BA emitter with a ridge width of 180 μm before and after BSPC. The insets (a,b) show, respectively, the beam spots before and after BSPC.

To obtain the details of beam quality, the M^2 factors were measured by using Thorlabs M^2 measurement systems (M2MS). Figure 3 shows the current dependent M^2 factors in the fast axis (M^2_y) and slow axis (M^2_x) of the laser with and without BSPC from 3 A to 8 A. The M^2_y of both devices were very close in the range from 1.1 to 1.28 and increased slowly with the increase of current. The small fluctuations in values were due to the measurement errors. Because the beam-waist splitting was along the slow axis, the improvement of beam quality happened only in slow axis and it was almost unchanged in the fast axis. In contrast, M^2_x increased with the current. The reasons behind this might be the high order mode operation due to the increased driving current [20] or the effect of lateral carrier accumulation [21]. When the driving current was 8 A, M^2_x was 18.45 under free running. After BSPC, it went down to 9.8, which corresponded to an improvement of 46%. BSPC achieved a significant beam quality improvement at little penalty of power. The M^2_x of the laser with BSPC was not as good as half of M^2_x with the same laser without BSPC, which was caused by the error of assembly and adjustment.

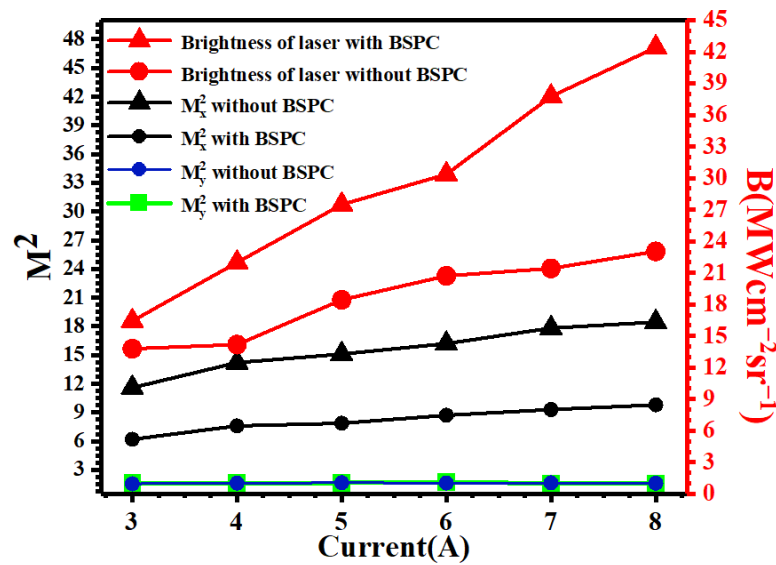


Figure 3. The dependence of M^2 factors and brightness B of the laser with and without BSPC on injection current.

Figure 3 also shows the brightness, B , of the single emitter with and without BSPC, which is defined as

$$B = \frac{P}{\lambda^2 M_x^2 M_y^2}, \tag{2}$$

where P is the power; λ is the center wavelength. It can be seen that the brightness B achieved by the single emitter without BSPC was about $23.01 \text{ MW cm}^{-2} \text{ sr}^{-1}$ at 8 A. For the same laser with BSPC, B increased to $42.4 \text{ MW cm}^{-2} \text{ sr}^{-1}$ at this injection current, which showed 84.21% improvement due to a better beam quality in the slow axis.

3.2. BSPC of BA Laser Bar

To check the applicability of the proposed BSPC method, the light source was replaced by a laser bar combined by SBC [15]. The schematic diagram of a set-up is shown in Figure 4. SBC is a simple and effective way to realize power scaling and increase spatial brightness greatly [22,23]. In SBC, a diode laser array (DA) was placed in an external cavity consisting of a transform lens (TL), a diffraction grating, and an output coupler (OC). After collimation in the fast and slow axis, the laser beams from the array focused on the grating by a transform lens. The OC fed the optical modes selected by the grating back to the laser array, and each emitter was forced to operate at a specific wavelength. The wavelength λ_i of each emitter can be expressed as:

$$\lambda_i = d \cdot \left[\sin(\theta_{\text{littrow}}) + \sin\left(\theta_{\text{littrow}} + \frac{i \cdot p}{f}\right) \right] \tag{3}$$

where d is the grating period; p represents the period of the emitters in the array; i is the number of the emitters along the SBC direction; and f is the focal length of the transform lens. Hence, the diode laser array was combined. After SBC, the brightness of the array can be further improved by BSPC.

The laser array was a standard centimeter 980 nm BAL bar with 19 emitters. The lateral emitter width was $90 \mu\text{m}$, and the vertical emitter width was $1 \mu\text{m}$. The FAC and SAC are commercial products with a focal length of 0.286 mm and 3 mm for the collimation of fast-axis and slow-axis, respectively. The transformation lens has an effective focal length of 450 mm, the grating has a groove density of 1800 lines/mm, and the diffraction efficiency is around 90%. The OC with 10% reflectivity was used.

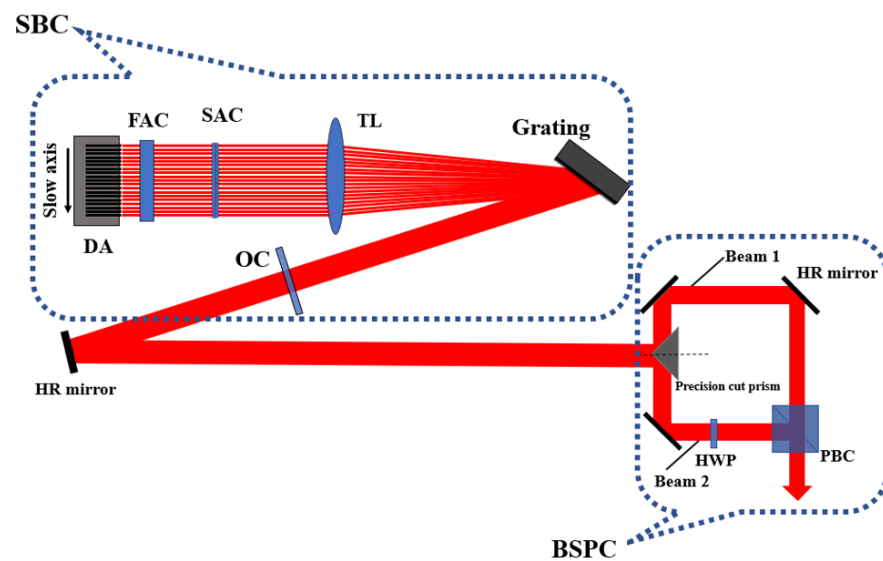


Figure 4. Schematic diagram of BSPC with SBC. DA: diode array. FAC: fast axis collimating lens. SAC: slow axis collimating lens. TL: transform lens. OC: output coupler.

Figure 5 shows the power-current characteristics of the SBC with (black balls) and without (red balls) BSPC under CW operation. The power was measured by Ophir FL500A at the coolant temperature of 18 °C. As can be seen, the output power of the SBC without BSPC at 36 A was 19.65 W. With the same current injection, the output power of the SBC with BSPC was 18.26 W, with only approximately a 7% loss.

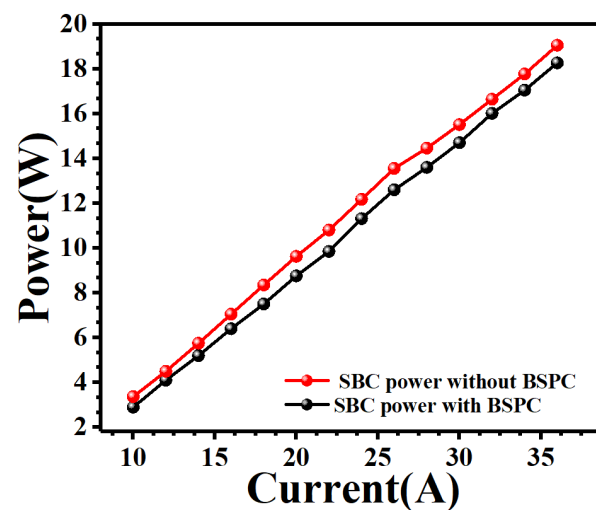


Figure 5. Optical power versus the injection current of the SBC with and without BSPC under continuous operation.

Beam quality and brightness of the single emitter with and without BSPC were also measured. Figure 6 shows the current dependent M^2 factors in the fast axis (M^2_y) and slow axis (M^2_x) of the SBC with and without BSPC from 10 A to 36 A. The M^2_y of both of these two setups were very close in the range from 2.02 to 2.07 and increased slowly with the increase of current. The fast axis beam quality did not change due to the introduction of BSPC. The M^2_x values of the two devices increased rapidly with the increase of current. The M^2_x of the SBC without BSPC increased from 4.78 to 9.08, and the M^2_y of the SBC with BSPC ranged from 2.35 to 4.75 with the same current injection. M^2_x of the laser with BSPC showed a 48% improvement. A significant beam quality improvement was achieved at the expense of little power by BSPC on SBC.

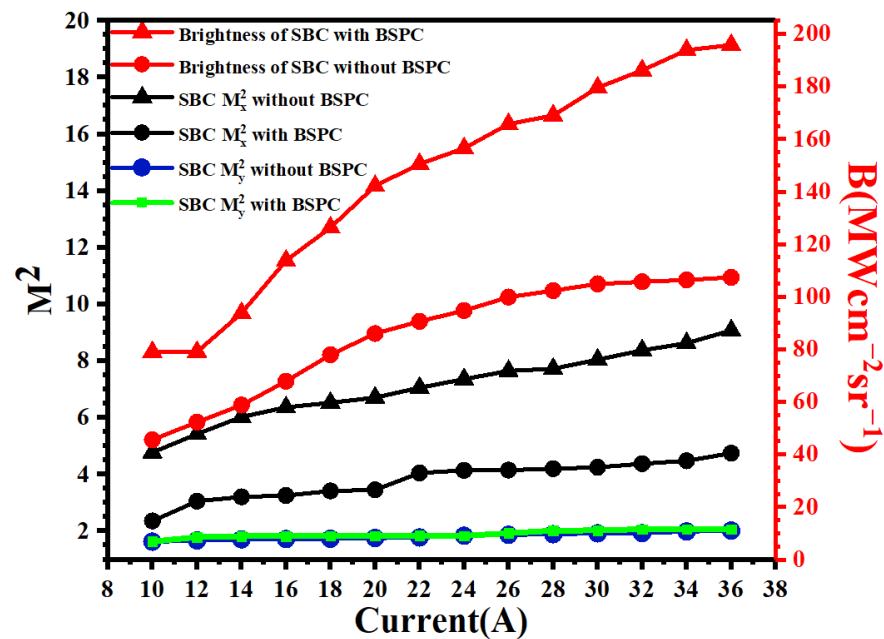


Figure 6. The dependence of M^2 factors and brightness of the SBC with and without BSPP on current.

Figure 6 also shows the brightness of the SBC with and without BSPP. It can be seen that the brightness B achieved by the SBC was about $108.4 \text{ MW cm}^{-2} \text{ sr}^{-1}$ at 36 A. The brightness increased to $195.8 \text{ MW cm}^{-2} \text{ sr}^{-1}$ by the same SBC with BSPP at this injected current, which corresponded to an improvement of 80.6%. The above results demonstrate that the proposed BSPP method was also suitable for the combined laser beam. The precondition is that the beam has the high purity of polarization.

4. Discussion

In summary, we demonstrated a new approach to enhance the brightness of a diode laser by beam-waist splitting and combining. It shows the noticeable advantages over the method based on reducing the divergence angle in the lateral direction [24–26], including the low power loss, significant brightness improvement, and simple device structure. The applicability of this approach was demonstrated in the diode laser of single emitter and laser array after combining. In total, 46% and 48% improvement of beam quality in slow axis were realized in these two types of laser sources with 9.5% and 7% power penalty. The brightness $42.4 \text{ MW cm}^{-2} \text{ sr}^{-1}$ and $195.8 \text{ MW cm}^{-2} \text{ sr}^{-1}$ were demonstrated in a single emitter and a commercial BA diode laser array combined by SBC. The brightness of these two types of laser source were enhanced 84.21% and 80.6%, respectively. We believe these results will contribute to the development of high brightness diode laser.

5. Patents

C.Z. Tong, Y.F. Zhao, F.Y. Sun, S.L. Shu, L. Wang, S.C. Tian, L.J. Wang, “Laser beam combining system,” US patent 10,768,434.

Author Contributions: Methodology, Y.Z.; validation, C.T. and Y.Z.; investigation, Y.Z. and L.W. (Lijie Wang); data curation, X.Z. and Y.W.; writing—review and editing, Y.Z. and C.T.; supervision, C.T. and Z.W.; project administration, C.T., L.W. (Lijun Wang) and H.L. All authors have read and agreed to the published version of the manuscript.

Funding: National Natural Science Foundation of China (Nos. 61790584, 62025506), and K.C. Wong Education Foundation (GJTD-2020-10).

Institutional Review Board Statement: Not applicable.

Informed Consent Statement: Not applicable.

Data Availability Statement: Not applicable.

Conflicts of Interest: The authors declare no conflict of interest.

References

1. Witte, U.; Schneider, F.; Traub, M.; Hoffmann, D.; Drows, S.; Brand, T.; Unger, A. kW-class direct diode laser for sheet metal cutting based on DWDM of pump modules by use of ultra-steep dielectric filters. *Opt. Express* **2016**, *24*, 22917–22929. [[CrossRef](#)] [[PubMed](#)]
2. Pietrzak, A.; Zorn, M.; Huelsewede, R.; Meusel, J.; Sebastian, J. Development of highly-efficient laser diodes emitting around 1060 nm for medical and industrial applications. *Proc. SPIE* **2019**, *10900*, 109000K. [[CrossRef](#)]
3. Shimada, N.; Yukawa, M.; Shibata, K.; Ono, K.; Yagi, T.; Shima, A. 640-nm laser diode for small laser display. *Proc. SPIE* **2009**, *7198*, 719806. [[CrossRef](#)]
4. Hakobyan, S.; Wittwer, V.J.; Brochard, P.; Gürel, K.; Schilt, S.; Mayer, A.S.; Keller, U.; Sudmeyer, T. Fully-Stabilized Optical Frequency Comb from a Diode-Pumped Solid-State Laser with GHz Repetition Rate. In Proceedings of the Conference on Lasers and Electro-Optics, OSA Technical Digest (Online) (Optical Society of America, 2017), San Jose, CA, USA, 14–19 May 2017. [[CrossRef](#)]
5. Yu, C.X.; Shatrovov, O.; Fan, T.Y.; Taunay, T.F. Diode-pumped narrow linewidth multi-kilowatt metalized Yb fiber amplifier. *Opt. Lett.* **2016**, *41*, 5202–5205. [[CrossRef](#)] [[PubMed](#)]
6. Sezer, H.; Tang, J.; Ahsan, A.N.; Kaul, S. Modeling residual thermal stresses in layer-by-layer formation of direct metal laser sintering process for different scanning patterns for 316 L stainless steel. *Rapid Prototyp. J.* **2022**. [[CrossRef](#)]
7. Ullah, A.; Rehman, A.U.; Salamci, M.U.; Pıtır, F.; Liu, T. The influence of laser power and scanning speed on the microstructure and surface morphology of Cu₂O parts in SLM. *Rapid Prototyp. J.* **2022**. [[CrossRef](#)]
8. Çalışkan, C.İ.; Arpacıoğlu, Ü. Additive manufacturing on the façade: Functional use of direct metal laser sintering hatch distance process parameters in building envelope. *Rapid Prototyp. J.* **2022**. [[CrossRef](#)]
9. Shaikh, M.Q.; Berfield, T.A.; Are, S.V. Residual stresses in additively manufactured parts: Predictive simulation and experimental verification. *Rapid Prototyp. J.* **2022**. [[CrossRef](#)]
10. Khorasani, M.; Ghasemi, A.; Rolfe, B.; Gibson, I. Additive manufacturing a powerful tool for the aerospace industry. *Rapid Prototyp. J.* **2022**, *28*, 87–100. [[CrossRef](#)]
11. Fuerschbach, P.W. Beam-quality measurements for materials processing lasers and the proposed ISO standard. *J. Laser Appl.* **1993**, *1993*, 312. [[CrossRef](#)]
12. Diehl, R. *High-Power Diode Lasers: Fundamentals, Technology, Applications*; Springer: Berlin/Heidelberg, Germany, 2000.
13. Zheng, Y.; Yang, Y.; Wang, J.; Hu, M.; Liu, G.; Zhao, X.; Chen, X.; Liu, K.; Zhao, C.; He, B.; et al. 108 kW spectral beam combination of eight all-fiber superfluorescent sources and their dispersion compensation. *Opt. Express* **2016**, *24*, 12063–12071. [[CrossRef](#)] [[PubMed](#)]
14. Wirth, C.; Schmidt, O.; Tsybin, I.; Schreiber, T.; Eberhardt, R.; Limpert, J.; Tünnermann, A.; Ludewigt, K.; Gowin, M.; Have, E.T.; et al. High average power spectral beam combining of four fiber amplifiers to 82 kW. *Opt. Lett.* **2011**, *36*, 3118–3120. [[CrossRef](#)] [[PubMed](#)]
15. Daneu, V.; Sanchez, A.; Fan, T.Y.; Choi, H.K.; Turner, G.W.; Cook, C.C. Spectral beam combining of a broad-stripe diode laser array in an external cavity. *Opt. Lett.* **2000**, *25*, 405–407. [[CrossRef](#)] [[PubMed](#)]
16. Huang, R.K.; Chann, B.; Missaggia, L.J.; Augst, S.J.; Connors, M.K.; Turner, G.W.; Sanchez-Rubio, A.; Donnelly, J.P.; Hostetler, J.L.; Miester, C.; et al. Coherent combination of slab-coupled optical waveguide lasers. In *Novel In-Plane Semiconductor Lasers VIII*; SPIE: San Jose, CA, USA, 2009; Volume 7230, pp. 292–303. [[CrossRef](#)]
17. Montoya, J.; Augst, S.J.; Creedon, K.; Kinsky, J.; Fan, T.Y.; Sanchez-Rubio, A. External cavity beam combining of 21 semiconductor lasers using SPGD. *Appl. Opt.* **2012**, *51*, 1724–1728. [[CrossRef](#)] [[PubMed](#)]
18. Liu, B.; Braiman, Y. Coherent addition of high power broad-area laser diodes with a compact VBG V-shaped external Talbot cavity. *Opt. Commun.* **2018**, *414*, 202–206. [[CrossRef](#)]
19. Tong, C.Z.; Zhao, Y.F.; Sun, F.Y.; Shu, S.L.; Wang, L.; Tian, S.C.; Wang, L.J. Laser Beam Combining System. US Patent 10,768,434, 8 September 2020.
20. Wang, L.; Tong, C.Z.; Shu, S.L.; Tian, S.C.; Sun, F.Y.; Zhao, Y.F.; Lu, H.Y.; Zhang, X.; Hou, G.Y.; Wang, L.J. Loss tailoring of high-power broad-area diode lasers. *Opt. Lett.* **2019**, *44*, 3562–3565. [[CrossRef](#)]
21. Winterfeldt, M.; Crump, P.; Knigge, S.; Maabdorf, A.; Zeimer, U.; Erbert, G. High Beam Quality in Broad Area Lasers via Suppression of Lateral Carrier Accumulation. *IEEE Photon. Technol. Lett.* **2015**, *27*, 1809–1812. [[CrossRef](#)]
22. Sun, F.Y.; Shu, S.L.; Hou, G.Y.; Wang, L.J.; Zhang, J.; Peng, H.Y.; Tian, S.C.; Tong, C.Z.; Wang, L.J. Efficiency and threshold characteristics of high-power diode lasers by spectral beam combining. *IEEE J. Quantum Electron.* **2019**, *55*, 2600107. [[CrossRef](#)]
23. Zhao, Y.F.; Sun, F.Y.; Tong, C.Z.; Shu, S.L.; Wang, L.J. Going beyond the beam quality limit of spectral beam combining of diode lasers in a v-shaped external cavity. *Opt. Express* **2018**, *26*, 14058. [[CrossRef](#)]
24. Rong, J.M.; Xing, E.B.; Zhang, Y.; Wang, L.J.; Shu, S.L.; Tian, S.C.; Tong, C.Z. Low lateral divergence 2 μm InGaSb/AlGaAsSb broad-area quantum well lasers. *Opt. Express* **2016**, *24*, 7246. [[CrossRef](#)]

25. Wang, L.J.; Tong, C.Z.; Tian, S.C.; Shu, S.L.; Zeng, Y.; Rong, J.M.; Wu, H.; Xing, E.; Ning, Y.Q.; Wang, L.J. High-power ultralow divergence edge-emitting diode laser with circular beam. *IEEE J. Sel. Top. Quantum Electron.* **2015**, *21*, 343–351. [[CrossRef](#)]
26. Wang, T.; Tong, C.Z.; Wang, L.J.; Wang, L.; Zeng, Y.; Tian, S.C.; Shu, S.L.; Zhang, J.; Wang, L.J. Injection-insensitive lateral divergence in broad-area diode lasers achieved by spatial current modulation. *Appl. Phys. Express* **2016**, *9*, 112102. [[CrossRef](#)]